Regenerative Therapy 24 (2023) 479–488

Contents lists available at ScienceDirect

Regenerative Therapy

journal homepage: http://www.elsevier.com/locate/reth

Original Article

Effect of morphological change on the maturation of human induced pluripotent stem cell-derived cardiac tissue in rotating flow culture

Akihiro Hashida [a], Taro Nakazato [b], Toshimasa Uemura [c, d], Li Liu [b], Shigeru Miyagawa [b], Yoshiki Sawa [e], Masahiro Kino-oka [a, *]

[a] Department of Biotechnology, Graduate School of Engineering, Osaka University, 2-1, Yamadaoka, Suita, Osaka, 565-0871, Japan
[b] Department of Surgery, Division of Cardiovascular Surgery, Graduate School of Medicine, Osaka University, 2-15, Yamadaoka, Suita, Osaka, 565-0871, Japan
[c] Department of Precise and Science Technology, Graduate School of Engineering, Osaka University, 2-1, Yamadaoka, Suita, Osaka, 565-0871, Japan
[d] Cell Culture Marketing & Research Center, JTEC Corporation, 2-1, Yamadaoka, Suita, Osaka, 565-0871, Japan
[e] Division of Health and Sciences, Graduate School of Medicine, Osaka University, 2-15, Yamadaoka, Suita, Osaka, 565-0871, Japan

ARTICLE INFO

Article history:
Received 17 June 2023
Received in revised form
6 August 2023
Accepted 4 September 2023

Keywords:
Human induced pluripotent stem cell-derived cardiac tissue
Rotating flow culture
Maturation
Tissue shrink
Nuclei shape
Spatial heterogeneity of tissue structure

ABSTRACT

Introduction: Understanding the critical factors for the maturation of human induced pluripotent stem cell (hiPSC)-derived cardiac tissue is important for further development of culture techniques. Rotating flow culture, where the tissues float in the culture medium by balancing its gravitational settling and the medium flow generated in rotating disk-shaped culture vessels, is one of culture systems used for tissue engineering. It has previously been demonstrated that rotating flow culture leads to the formation of matured cardiac tissue with higher levels of function and structure than the other culture systems. However, the detailed mechanisms underlying the maturation of cardiac tissue remain unclear. This study investigated the maturation process of hiPSC-derived cardiac tissue in rotating flow culture with a focus on morphological changes in the tissue, which is a trigger for maturation.
Methods: The cardiac tissue, which consisted of cardiomyocytes derived from hiPSCs, was cultured on the 3D scaffold of poly (lactic-*co*-glycolic) acid (PLGA)-aligned nanofibers, in rotating flow culture for 5 days. During the culture, the time profile of projected area of tissue and formation of maturation marker proteins (β-myosin heavy chain and Connexin-43), tissue structure, and formation of nuclear lamina proteins (Lamin A/C) were compared with that in static suspension culture.
Results: The ratio of the projected area of tissue significantly decreased from Day 0 to Day 3 due to tissue shrinkage. In contrast, Western blot analysis revealed that maturation protein markers of cardiomyocytes significantly increased after Day 3. In addition, in rotating flow culture, flat-shaped nuclei and fiber-like cytoskeletal structures were distributed in the surface region of tissue where medium flow was continuously applied. Moreover, Lamin A/C, which are generally formed in differentiated cells owing to mechanical force across the cytoskeleton and critically affect the maturation of cardiomyocytes, were significantly formed in the tissue of rotating flow culture.
Conclusions: In this study, we found that spatial heterogeneity of tissue structure and tissue shrinkage occurred in rotating flow culture, which was not observed in static suspension culture. Moreover, from the quantitative analysis, it was also suggested that tissue shrinkage in rotating flow culture contributed its following tissue maturation. These findings showed one of the important characteristics of rotating flow culture which was not revealed in previous studies.

1. Introduction

Human induced pluripotent stem cell (hiPSC)-derived cardiomyocytes are promising sources for basic biological research and for clinical applications, such as regenerative medicine and/or

* Corresponding author.
E-mail address: kino-oka@bio.eng.osaka-u.ac.jp (M. Kino-oka).
Peer review under responsibility of the Japanese Society for Regenerative Medicine.

https://doi.org/10.1016/j.reth.2023.09.002

drug screening [1,2]. Various differentiation methods have been developed to obtain a large number of cardiomyocytes [3–5]. In addition, tissue engineering technologies for hiPSC-derived cardiomyocytes have been improved, enabling the fabrication of three-dimensional (3D) cardiac tissue using a multi-layer cell sheet technique [6] and/or scaffold technique [7]. After constructing 3D cardiac tissue, maturation culture of the tissue is generally performed to obtain higher levels of structure and function, such as sarcomere structure (for generation of contractile force; cardiac troponin T (cTnT), sarcomeric alpha-actinin (SAA),β-myosin heavy chain (β-MHC)) [8–10], cell-cell gap junctions (for synchrony of beating; Connexin-43) [11], higher cell alignment (for effective transmission of contractile force) [12,13], metabolism (for supporting the generation of contractile force) [14–16], etc. Several culture methods for tissue maturation, have been developed for supplying sufficient oxygen and nutrients by providing hydrogel [17] and/or vascular networks [18], giving mechanical stress [19–21], and improving cell alignment [22]. These culture methods can be realized both in the static suspension and perfusion culture systems [23–25]. It is also important to understand the critical factors that affect tissue maturation in each culture system for further development of cardiac tissue engineering.

Rotating flow culture is one of culture systems for tissue engineering developed by the National Aeronautics and Space Administration (NASA) in the 1970s [26–28]. In this culture system, the tissues float in the culture medium by balancing its gravitational settling and upper medium flow generated in a rotating disk-shaped culture vessel (Movie S1) [26–28]. This unique characteristic has been used for various types of tissue cultures, such as hepatic tissue [29,30], bone tissue [31], and cartilage tissue [32,33], and it has also been reported that tissues with higher levels of structure and function could be obtained in this culture system. For 3D cardiac tissue culture, Nakazato et al. [34] demonstrated the utility of a rotating flow culture system for obtaining more mature cardiac tissue with a thicker structure than the tissue cultured in static suspension culture. Moreover, they also found that the signaling pathways associated with cell-substrate adhesion and survival (integrin and focal adhesion kinase (FAK)), and physiological hypertrophy, which can indicate the maturation of cardiac tissue (mTORC1 and S6K) [35,36], were significantly activated compared with those in static suspension culture [34]. From these results, Nakazato et al. [34] concluded that physiological hypertrophy is an important phenomenon for tissue maturation in rotating flow culture, but the critical factors in this culture system that trigger this phenomenon remain unclear.

Supplementary video related to this article can be found at https://doi.org/10.1016/j.reth.2023.09.002

Generally, with the maturation of cardiomyocytes, sarcomere structures consisting of actin filaments, myosin mortars, and other cytoskeletal proteins are formed, resulting in the generation of contractile force for beating and its synchrony [8–11]. In addition, these cardiomyocytes were observed to be elongated in shape to transmit contractile force more effectively between neighboring cells [37,38]. This resulted in morphological and structural changes in 3D cardiac tissue. Therefore, it is essential to understand the factors that trigger the formation and functional improvement of sarcomere structure. Mechanical force is a major factor that affects the sarcomere structure formation [19–21]. It is also known that, as one of mechanisms, the mechanical force regulates several factors promoting sarcomere structure via the nuclear lamina formation [39]. In the case of rotating flow culture, where medium flow balanced with gravitational settling continuously apply to the tissue, there should be critical factors associated with nuclear lamina, but the detail mechanism is still unclear. In this study, we investigated the maturation process of hiPSC-derived cardiac tissue in rotating flow culture with a focus on its morphological changes, which might be a key factor for transmitting mechanical force to the tissue resulting in maturation.

2. Materials and methods

2.1. Aligned nanofibers fabrication

The aligned nanofibers were prepared as described previously (Fig. S1) [21,34]. For 3D fibers scaffold fabrication, Co-polymer material, PLGA (75/25; Sigma-Aldrich, St. Louis, MO, USA), was dissolute in hexafluoro-2-propanol (HFIP, Wako Pure Chemical Industries, Tokyo, Japan) (1.2 g:3 mL, w/v). And then, the fibers were fabricated by using an electrospinning machine (NF-103, MECC, Fukuoka, Japan). The solution was loaded into a 3-mL syringe with a needle of 0.6-mm inner diameter. The positive electrode of the high-voltage power supply (10 kV), and the distance between the needle and the collector was kept at 15 cm. A layer of aluminum foil was attached to the grounded drum. The drum was rotated at a speed of 1000 rpm for collecting the fiber. Finally, the fiber sheet was transferred to a PDMS frame (6 mm × 6 mm) for cell culture.

2.2. Cells and culture conditions

Human induced pluripotent stem cells (hiPSCs) (253G1 line, RIKEN Bio-resource Center, Tsukuba, Japan) were routinely maintained on polystyrene culture dishes coated with Repro Coat (Repro CELL Inc., Tokyo, Japan) by coculturing with mitomycin C-treated mouse embryonic fibroblasts (MEFs) (Repro CELL Inc.) in commercially available media (Primate ES Cell Medium) (Repro CELL Inc.) containing 5 ng mL^{-1} basic fibroblast growth factor (bFGF) (Repro CELL Inc.). Cells were passaged every 5 days, and the media were changed daily. For preparation of feeder layers, mitomycin C-treated MEFs were seeded at a density of 1.4×10^4 cells cm^{-2} on culture surface coated with Repro Coat and cultivated for 1 day in Dulbecco's modified Eagle's medium (DMEM) (Nacalai Tesque Co. Ltd., Kyoto, Japan) supplemented with 10% fetal bovine serum (FBS) (Thermo Fisher Scientific, Waltham, MA, USA) and 1% penicillin–streptomycin (Thermo Fisher Scientific). For passages of hiPSCs, feeder cells were removed after incubation with dissociation solution (Repro CELL Inc.) for 5 min. The hiPSC colonies in the undifferentiated state were carefully collected, and the suspension of collected undifferentiated colonies was pipetted gently for dispersal into small aggregates and then dispensed into a fresh culture vessel containing feeder cells. The medium was replaced daily with fresh medium.

2.3. Cardiac differentiation culture of hiPSCs

Cardiac differentiation culture of hiPSCs was conducted as described previously [40]. For the differentiation culture, Stempro-34 (Thermo Fisher Scientific) supplemented with 2 mM L-glutamine (Thermo Fisher Scientific), 50 μg mL^{-1} ascorbic acid (FUJIFILM Wako Pure Chemical Industries, Osaka, Japan), and 400 μM 1-thioglycerol (Sigma) was used as the culture medium. On Day 0, the hiPSCs and MEFs were treated with Accumax (Innovative Cell Technologies Inc., San Diego, CA, USA) containing 10 μM Culture Sure Y-27632 (FUJIFILM Wako Pure Chemical Industries) for 10 min at 37 °C, 5% CO_2, and dissociated into single cells. After centrifugation (1000 rpm, 3 min, room temperature), the cells were resuspended into single cells with culture medium containing 5 μM Culture Sure Y-27632 and 5 ng mL^{-1} bone morphogenetic protein 4(BMP-4) (R&D Systems, USA) and seeded into a 30 mL bioreactor

(ABLE Co. Ltd., Tokyo, Japan) at a seeding density of 1.5×10^5 cells mL^{-1}. The following growth factors and small molecules were used on the corresponding days: Day 1–4, 10 ng mL^{-1} BMP-4, 5 ng mL^{-1} bFGF, 14 ng mL^{-1} activin A (R&D Systems, USA); Day 4–6, 6 μM IWR-1(Sigma), 8 μM IWP-2 (Sigma, St Louis, MO, USA); after Day 6, 5 ng mL^{-1} VEGF (FUJIFILM Wako) and 10 ng mL^{-1} bFGF. On days 4, 6, 8, 10, 12, and 14, the culture medium was replaced. On Day 15, the cell aggregates were collected and treated with 0.05% trypsin/EDTA (Thermo Fisher Scientific) and HBSS (Sigma) for 10 min at 37 °C. After enzymatic treatment, the cell aggregates were dissociated into single cells by pipetting and these cells were used for flow cytometry analysis and cardiac tissue culture.

2.4. Flow cytometry

The dissociated cells were fixed and permeabilized using Cytofix/Cytoperm (BD) for 30 min at 4 °C. After fixation and permeation, the cells were incubated in 0.5% Bovine Serum albumin under 4 °C overnight for blocking. On the next day, the cells were resuspended in a buffer containing 2 μg mL^{-1} anti-cardiac troponin T antibody conjugated with Alexa Fluor 488 (Santa Cruz Biotechnologies) for 1 h at 4 °C. After the antibody reaction, the cells were washed and analyzed using a flow cytometer (Cube 6; Sysmex, Hyogo, Japan) to detect the ratio of cardiac troponin T-positive cells. The ratio of troponin T positive cells for cardiac tissue culture was 81.3 ± 2.6% ($n = 6$) in this study.

2.5. Cardiac tissue culture

Cardiac tissue culture was conducted based on previously described methods (Fig. 1) [34]. The dissociated cells were resuspended in DMEM containing 10% FBS, 1% penicillin–streptomycin, 10 μM Culture Sure Y-27632 and 10 μg mL^{-1} Laminin-511 E8 fragments (iMatrix-511; Nippi, Tokyo, Japan) at cell density 3.3×10^7 cells mL^{-1}. The cell suspension of 2.0×10^6 cells was seeded on 6 mm × 6 mm aligned nanofibers [22] and incubated at 37 °C, 5% CO_2 for 3 h. After incubation, 5 mL DMEM/10% FBS/1% penicillin–streptomycin was added and pre-culture was initiated. After 3 days of pre-culture, the cardiac tissue was cultured under static and floating conditions using a rotating flow culture system (Cell Float System, JTEC Corporation, Osaka, Japan) for 5 days. The culture vessels were filled with 65 mL $vessel^{-1}$ of DMEM/10% FBS/1% penicillin–streptomycin, and their rotational speeds of culture vessels were 0 and 10 rpm under static and floating conditions, respectively.

2.6. Observation of cardiac tissue morphology

To observe tissue morphology, cardiac tissues were collected on days 0, 1, 3, and 5, and bright-field images were captured using a 2 × objective lens in the image analyzer (IN Cell Analyzer 2000; GE Healthcare, Chicago, IL, USA). The projected area of tissue, S (μm^2), was determined using image processing software (Image-Pro Plus 7.0; Media Cybernetics Inc., Rockville, MD, USA), as described previously [41].

2.7. Western blotting

Protein extraction and Western blot analysis were conducted as previously described [42,43]. Whole-cell proteins were extracted from cultured cells using RIPA lysis buffer (Sigma) supplemented with a protease and phosphatase inhibitor cocktail (Thermo Fisher Scientific). Proteins were separated by sodium dodecyl sulfate-polyacrylamide gel electrophoresis and then transferred to polyvinylidene difluoride membranes (Bio-Rad). After blocking with 5% ECL blocking agent (GE Healthcare) in TBS, the membranes were probed with the following primary antibodies overnight at 4 °C: anti-cardiac troponin T antibody, anti-sarcomeric alpha-actinin antibody, anti-Lamin B1 antibody (Abcam, Cambridge, MA, USA), anti-myosin heavy chain 7 (MYH7) (type I) (Proteintech, Manchester, UK), anti-Connexin-43 antibody (Sigma), anti-Lamin A/C antibody (Santa Cruz Biotechnology, Inc., Santa Cruz, CA, USA), and anti-glyceraldehyde-3-phosphate (GAPDH) antibody (Cell Signaling Technology Inc., Danvers, MA, USA), washed with TBS containing 0.1% Tween-20 (TBST), and incubated with fluorescent dye-conjugated secondary antibodies (Bio-Rad) for 1 h at room temperature. After washing with TBST, the protein bands on the immunoblots were detected using infrared fluorescence with a ChemiDoc MP imaging system (Bio-Rad). The signal intensity of each band was quantified using an image analysis software (Image Lab; Bio-Rad). GAPDH and Lamin B1 were used as the internal controls for sample loading.

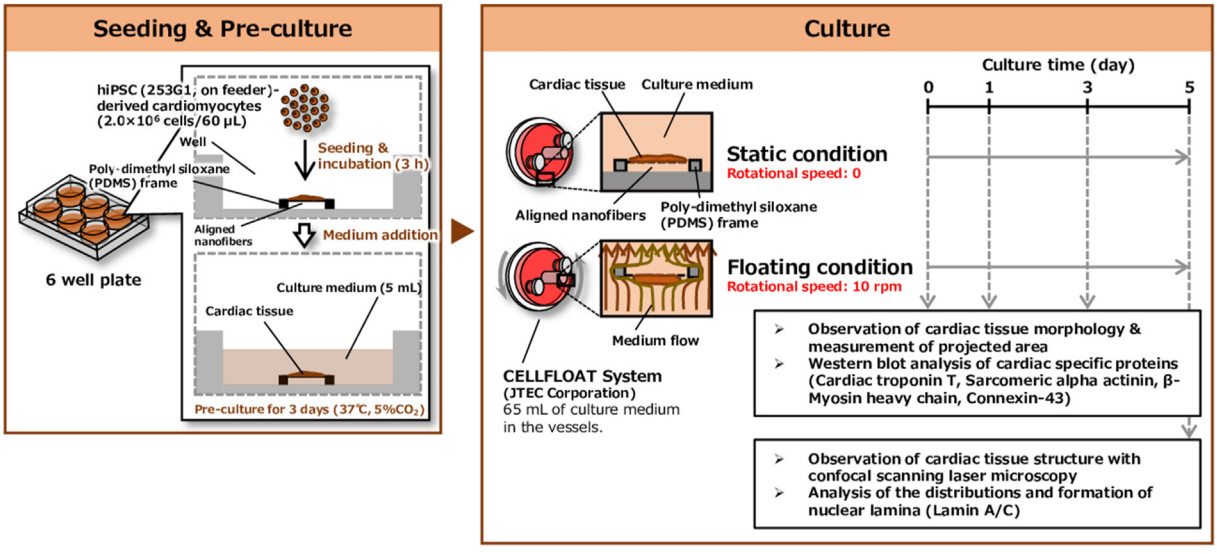

Fig. 1. The procedure for the culture of cardiac tissue under static and floating conditions.

2.8. Fluorescence staining

To observe tissue structure, fluorescence staining of frozen tissue sections was conducted as previously described [42,43]. On Day 5, the tissues were rinsed with phosphate-buffered saline (PBS) and fixed with 4% paraformaldehyde (FUJIFILM Wako Pure Chemical Industries) for 30 min at room temperature. After treatment with 15% sucrose/PBS overnight at 4 °C, the tissues were embedded in optical cutting temperature (OCT) compound (Tissue-Tek, Sakura Finetek Japan Co., Ltd.). Frozen sections (60 and 10 μm) were prepared using a cryostat microtome (Leica CM1850). The sections were rinsed with PBS and permeabilized with 0.5% Triton-X-100/PBS for 10 min at room temperature.

For 3D structure observation, 60 μm tissue sections were stained with 40,6-diamidino-2-phenylindole (DAPI; Life Technologies) and Alexa 488 conjugated phalloidin (Thermo Fisher Scientific) for 2 h at room temperature. After washing the sections with PBS, the specimens were observed under a confocal laser scanning microscope (FV1000; Olympus, Tokyo, Japan). For immunostaining, 10 μm sections were blocked in Block Ace (Dainippon Sumitomo Pharma Co., Ltd.) for 90 min at RT. Subsequently, sections were incubated with the following primary antibodies overnight at 4 °C in PBS containing 10% Block Ace: anti-Lamin A/C antibody (Santa Cruz Biotechnology, Inc.) and anti-Lamin B1 antibody (Abcam). Sections were then washed twice with Tris-buffered saline (TBS; Dako Japan Inc., Tokyo, Japan) and immersed in PBS containing 10% Block Ace and Alexa Fluor 594-conjugated goat anti-mouse secondary antibody (A11005, Life Technologies), Alexa Fluor 488-conjugated donkey anti-goat secondary antibody (A11055, Life Technologies), and Alexa Fluor 488-conjugated goat anti-rabbit secondary antibody (A11008, Life Technologies), respectively, for 60 min at room temperature. The cell nuclei were stained with 40,6-diamidino-2-phenylindole (DAPI; Life Technologies) for 20 min. The specimens were observed under a confocal laser scanning microscope (FV1000; Olympus, Tokyo, Japan).

2.9. Statistical analysis

At least three independent experiments were conducted for each tested condition. The data are expressed as means ± standard deviations. Statistical comparisons were performed using Student's *t*-test, and values of $p < 0.01$ and $p < 0.05$ were considered significant.

3. Results

3.1. Time-dependent change in tissue morphology

The change in tissue morphology was studied under static and floating conditions for over a period of 5 days. We compared the ratio of projected area of tissue on days 1, 3, and 5 against that on Day 0 between static and floating conditions. Fig. 2A shows the time profile of S/S_0 (−), where S (μm^2) is the projected area of the tissue on days 1, 3, and 5, and S_0 (μm^2) is the projected area of the tissue on Day 0. The value of S/S_0 (−) under the floating condition

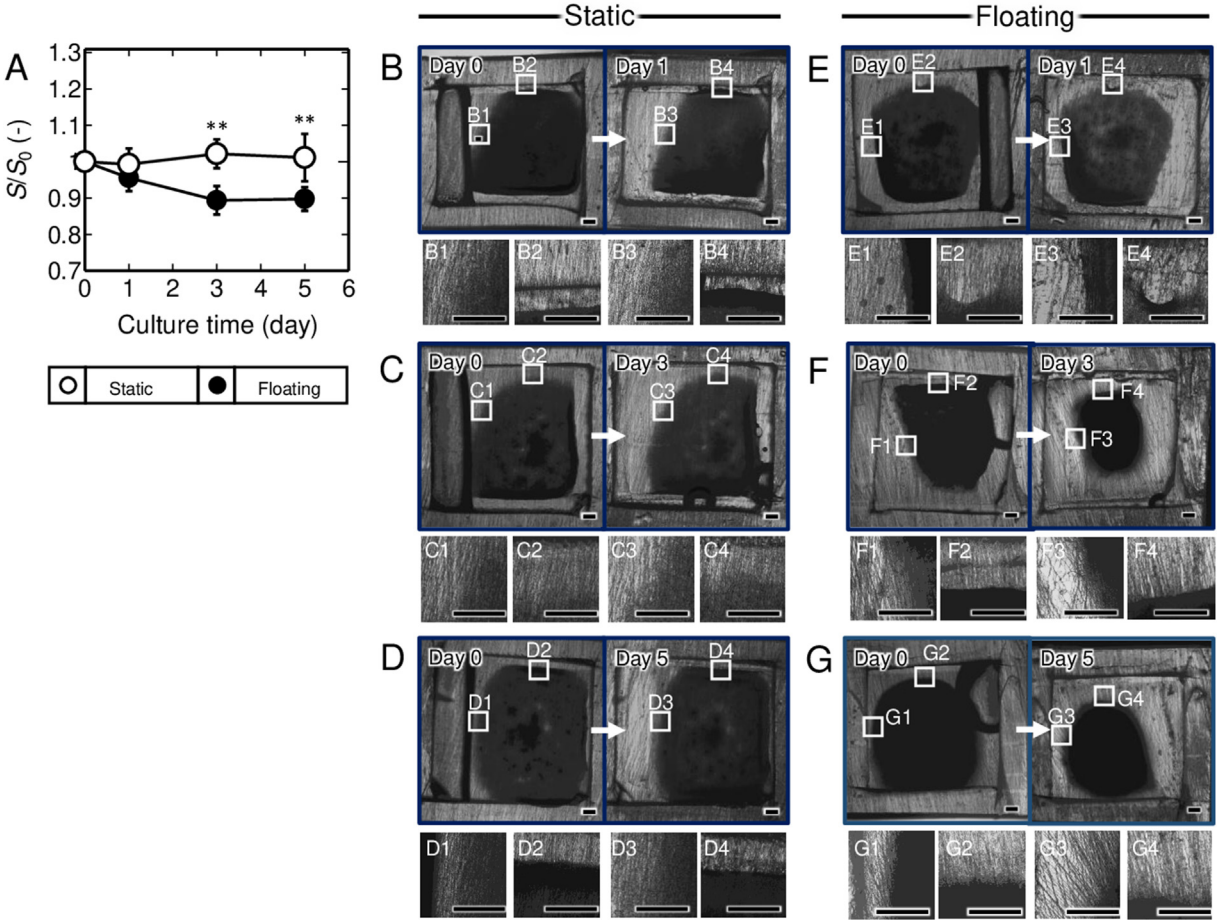

Fig. 2. Morphological changes in cardiac tissue under static and floating conditions. (A) Time profile of the projected area ratio (S/S_0). Statistical significance was determined by performing two-tailed Student's *t*-tests: $*p < 0.05$, $**p < 0.01$ ($n = 6$). Error bars represent the standard deviation. (B–G) Bright-field images of cardiac tissue on days 0, 1, 3, and 5 under static (B–D) and floating conditions (E–G). Scale bars show 500 μm.

significantly decreased from Day 0 to Day 3, whereas that under the static condition remained constant. From the bright-field images of the cardiac tissue (Fig. 2B–G), a significant difference was observed between static and floating conditions, especially on Day 3 and Day 5 (Fig. 2C, D, F, and G). The cardiac tissue under static condition on Day 3 and Day 5 showed similar morphology to that on Day 0, whereas the tissue under the floating condition was observed to be shrunk.

3.2. Formation of cardiac-specific proteins in the tissue

Maturation of the cardiac tissue can be identified by the presence of cardiac-specific protein markers. We investigated the formation of cardiac-specific proteins (cardiac troponin T (cTnT), sarcomeric alpha-actinin (SAA), β-myosin heavy chain (β-MHC), and Connexin-43) by western blotting, as per the method described previously [34]. Fig. 3 shows Western blot images and quantitative analysis. For quantitative analysis, we first calculated the relative intensity of each protein against GAPDH. The normalized intensity in Fig. 3B–E is their relative values when those on Day 0 were 1. We found that the formation of β-MHC and Connexin-43 under the floating condition significantly increased after Day 3, whereas that under the static condition remained constant (Fig. 3A, D, and E). In contrast, the intensity levels of cTnT and SAA under static and floating conditions remained constant with no significant differences (Fig. 3A–C).

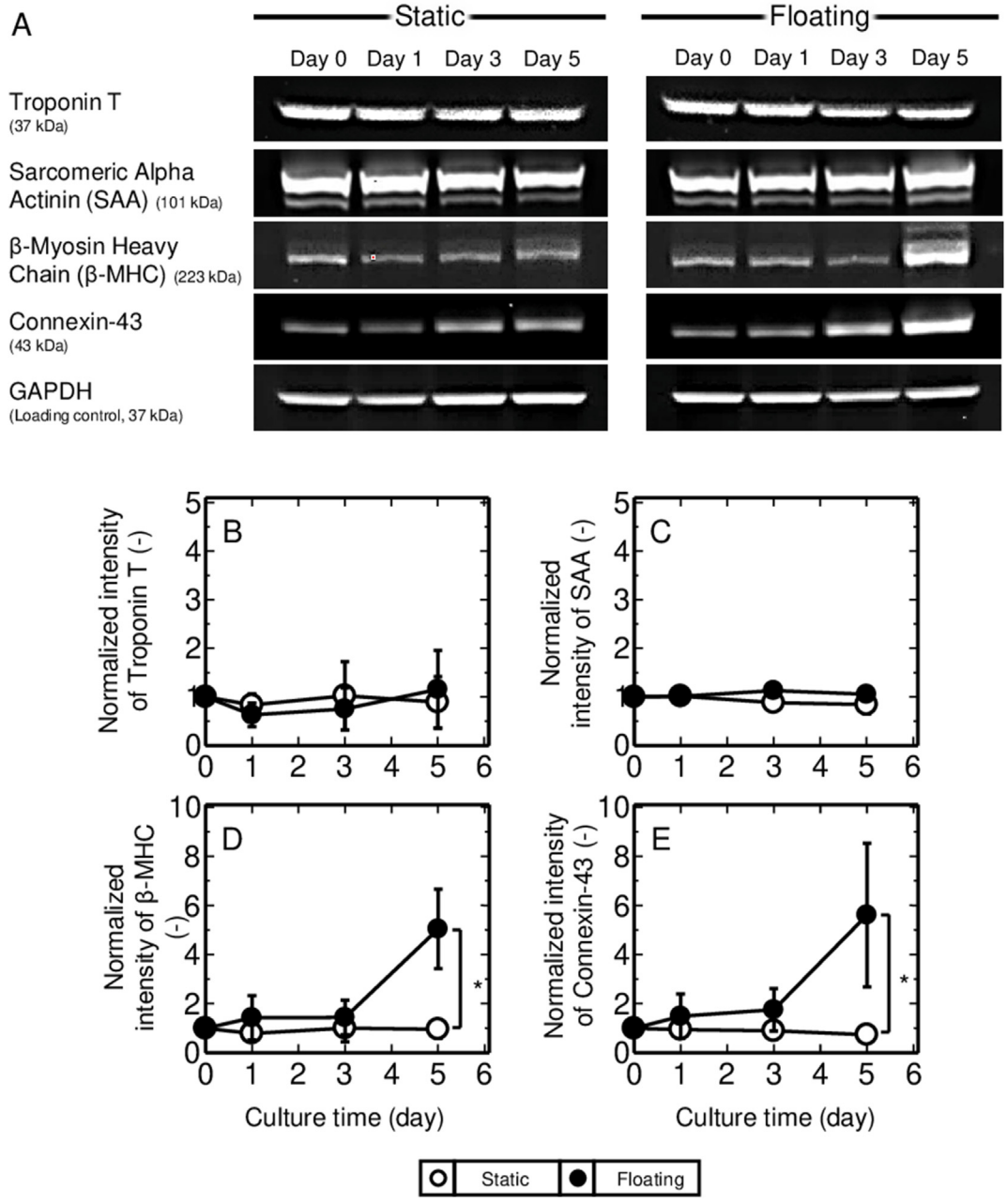

Fig. 3. Maturation properties of cardiac tissue under static and floating conditions. (A) The Western blot images of cardiac troponin T, sarcomeric alpha-actinin (SAA), β-myosin heavy chain (β-MHC), Connexin-43, and glyceraldehyde-3-phosphate (GAPDH) (loading control), and (B–E) their quantitative analysis. The intensity of each target proteins was normalized to that of GAPDH. Open circle: static condition, closed circle: floating condition. Statistical significance was determined by performing two-tailed Student's *t*-tests: $*p < 0.05$, $**p < 0.01$ ($n = 3$).

3.3. Characteristics of tissue structure cultured in rotating flow culture

Further, to understand the characteristics of nuclei shape in the tissue cultured under floating conditions, we performed 3D observation of the frozen sections of tissue using a confocal laser scanning microscope and compared the structure with that of the static condition. Fig. 4 shows fluorescence images of tissue sections captured in the central and peripheral regions of the tissue. Moreover, Fig. 4A1-D3 show magnified and 3D views of the boxed area in Fig. 4A–D; the fiber sheet side, middle side, and surface side of the tissue. We determined the position of aligned nanofibers in the tissue based on the entire field images (data are not shown), and defined the position as “fiber sheet side”. We also defined the opposite side of the fiber sheet side as “surface side”, and the position between fiber sheet side and surface side as “middle side”.

We observed differences in the tissue structure between static and floating conditions in the central and peripheral regions. The tissues under the static condition were thinner and had flatter structures in the central and peripheral regions, respectively, while those under the floating condition were thicker and rounder structures (Fig. 4A–D). In addition, we also found a significant difference in nuclei shape, especially on the peripheral region of the tissue, between static and floating conditions. The nuclei under the static condition showed a round shape (Fig. 3A3 and B3), while those under the floating condition showed a flat shape (white head arrows) (Fig. 4C3 and D3). Moreover, we also found that F-actin on the surface side of the floating condition showed a fiber-like structure along the tissue surface (Fig. 4C3 and D3), while that under the static condition showed a non-fiber-like structure (Fig. 4A3 and B3).

3.4. Formation of nuclear lamina in cardiac tissue

To identify the key factors of cardiac maturation in the tissue, we also investigated the distribution and formation of nuclear lamina in the tissue based on the methods described in the previous studies [42,43]. Immunostaining images showed that nuclear lamina (Lamin A/C) positive cells were more often identified in the tissue cultured under the floating condition than under the static condition (Fig. 5A). Moreover, based on Western blot analysis, the formation of Lamin A/C under floating conditions was higher than that under static conditions (Fig. 5B, C).

4. Discussion

We investigated the maturation process of cardiac tissue in rotating flow culture, focusing on the morphological changes in the tissue, which could trigger maturation. We identified the important characteristics in the time-dependent change in tissue morphology and cardiac-specific protein formation. We hypothesized that the key factors for cardiac maturation could be attributed to the morphological changes in the tissue. Based on our findings, the possible process involved in cardiac tissue maturation mediated by morphological and structural changes in the tissue cultured under rotating flow culture is illustrated in Fig. 6.

First, we identified the important characteristics of morphological changes in tissues. As shown in Fig. 2, the value of S/S_0 under

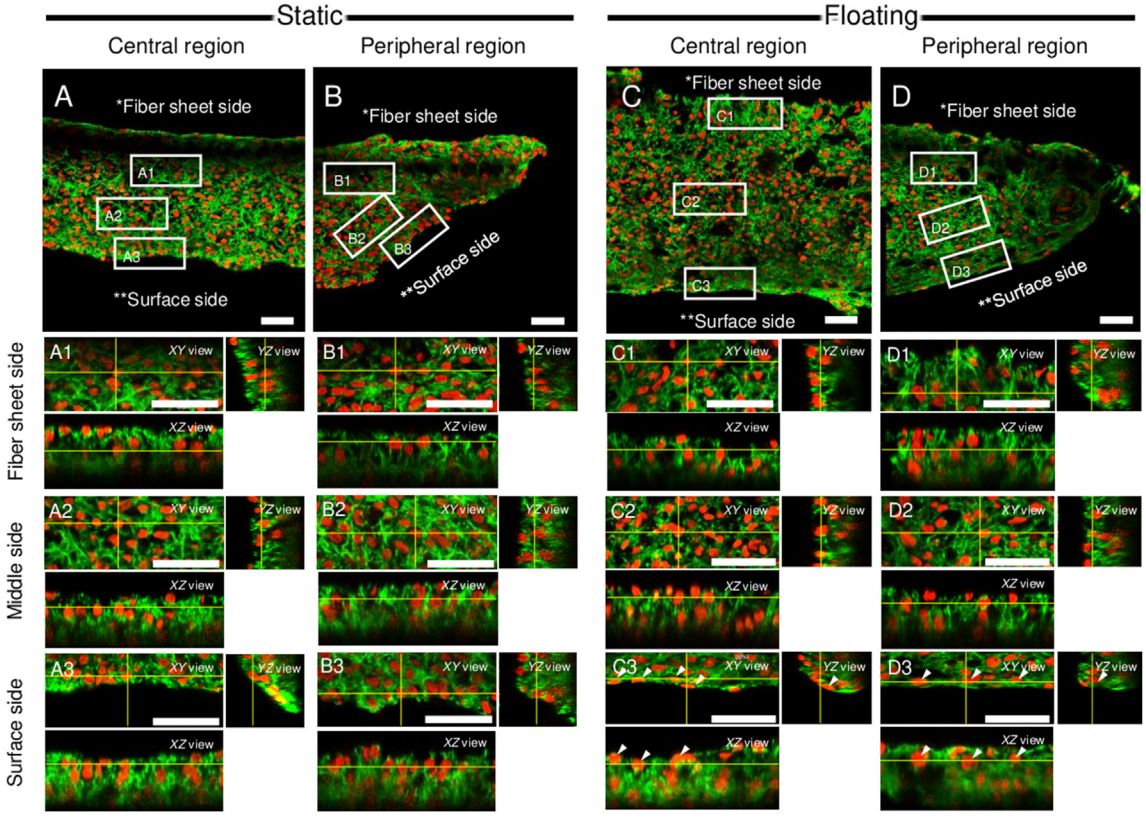

Fig. 4. Localization of nuclei and actin cytoskeleton in human induced pluripotent stem cell (hiPSC)-derived cardiac tissue cultured under static (A, B) and floating (C, D) conditions on Day 5. Confocal fluorescence images of F-actin (green) and nuclei (red) show top-down views of 3D-reconstruction (XYZ planes) and 2D optical cross-sectioning (XZ and YZ planes) (A1–A3, B1–B3, C1–C3, and D1–D3). The yellow lines in the top-down views indicate the location of the cross-sectional side view. White head arrows (C3 and D3) show flat-shaped nuclei. Scale bars = 50 μm.

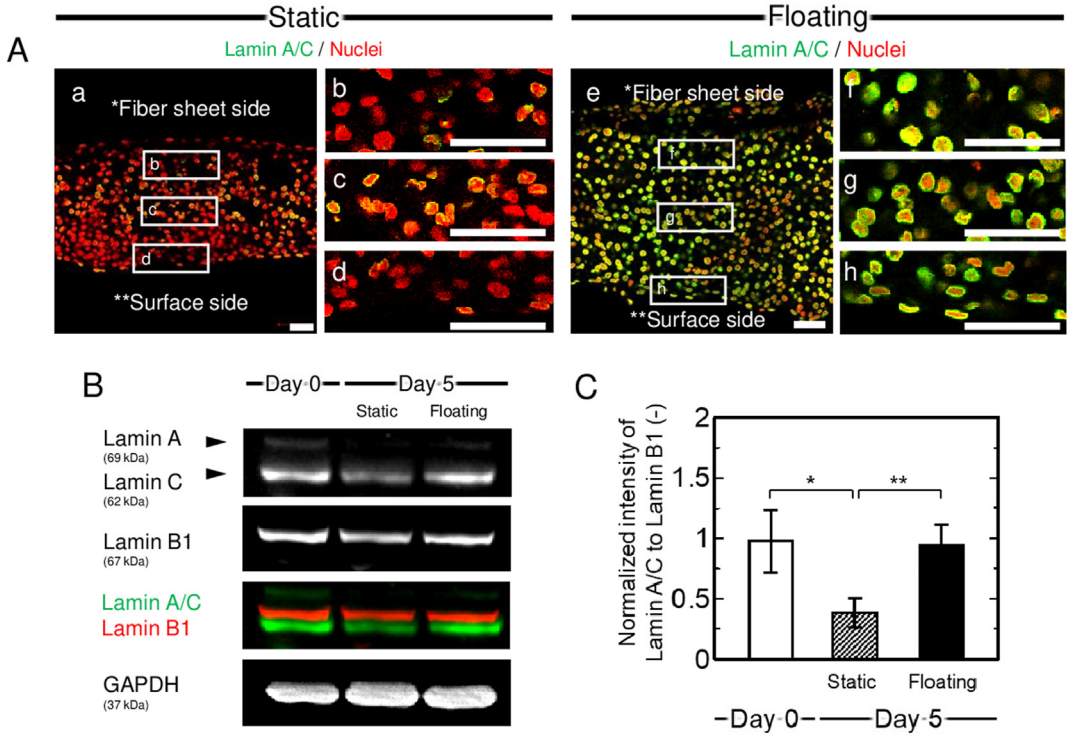

Fig. 5. Distribution and formation of nuclei lamina in cardiac tissue under static and floating conditions. (A) Immunostaining images of Lamin A/C (green) and nuclei (red) in the central region of cardiac tissue. (b-d, f-h) Magnified views of the boxed area in (a) and (d), respectively. Scale bars show 50 μm. (B) The Western blot images of Lamin A/C, Lamin B1, and glyceraldehyde-3-phosphate dehydrogenase (GAPDH) and (C) their quantitative analysis. The intensity of each target proteins was normalized to that of GAPDH. Open bar: Day 0, hatched bar: static condition on Day 5, and closed bar: floating condition on dat 5. Statistical significance was determined by performing two-tailed Student's *t*-tests: $*p < 0.05$, $**p < 0.01$ ($n = 3$).

floating condition significantly decreased from Day 0 to Day 3, whereas that under the static condition remained constant. Moreover, it was also confirmed that the tissue cultured in the floating condition showed a thicker structure compared with that in the static condition (Fig. 4A–D). Considering that the fiber sheet structure wound, especially on Day 3 and Day 5 (Fig. 2F and G), it is suggested that the tissue shrunk to become thicker structure from Day 0 to Day 3, and that the tissue maintained its structure after Day 3. In addition, the formation of cardiac-specific proteins β-MHC and Connexin-43 significantly increased after Day 3 (Fig. 3D and E), suggesting that tissue maturation was initiated after tissue shrinkage (Fig. 6).

Generally, contractile force in cardiomyocytes is generated by a sarcomere structure consisting of actin, myosin, and other cytoskeletal proteins [8–10]. The maturation of cardiomyocytes is initiated by the formation and alignment of these cytoskeletal proteins, and the morphological, metabolic, and other functional changes in the cells follow this process to provide stronger and more synchronized contractile force to cardiomyocytes [10]. Further, it is considered that this maturation process is induced by two factors: the contractile force generated by themselves [44], and the mechanical force provided by the external environment [19–21]. The former process is realized by vinculin molecules in the cells, which assemble in the desmosome when contractile force occurs and consequently recruit Slingshot protein phosphatase 1 (SSH1) to activate cofilin, leading to myofilament rearrangement of cardiomyocytes [44]. Under both static and floating conditions, the cardiomyocytes beat due to the contractile force generated by themselves, and it can be speculated that there might be no significant difference in this process among the two conditions. Therefore, other external forces in rotating flow culture should induce tissue shrinkage and maturation. We analyzed the tissue structure to determine the relationship between tissue structure and culture environment.

The results of tissue structure observation under floating condition showed different characteristics in nuclei shape and F-actin structure from that of static condition (Fig. 4). Round-shaped nuclei homogeneously distributed under static conditions (Fig. 4A and B), whereas flat-shaped nuclei and fiber-like F-actin structure were confirmed, especially in the surface side of the tissue under floating conditions, where medium flow was continuously applied (Fig. 4C3 and D3). It is considered that the cells in the surface side were compressed from the outside to the inside of the tissue owing to the medium flow. From the previous studies, it is known that the effect of fluid shear stress on the alignment of the cytoskeleton in myocytes, and it was suggested that the cytoskeletal proteins aligned along the direction of shear stress [37,38]. Further, Nakano et al. [45] reported that the compression of cardiomyocyte aggregates enhances the contractile force generated in cardiomyocytes. Under floating conditions, medium flow was vertically applied to the surface of the tissue, and it is considered that the cells on the surface region might be compressed owing to medium flow. In addition, the shear stress of the medium flow was also might have applied to the tissue along the tissue surface, and it is speculated that the alignment of cytoskeletal proteins improved and a stronger contractile force along the tissue surface was generated compared with that under static conditions, which resulted in tissue shrinkage.

We also found that the formation and distribution of nuclear protein, Lamin A/C were markedly different between static and floating conditions. Generally, Lamin A/C is formed inside the nuclei of differentiated cells when they receive mechanical stress from

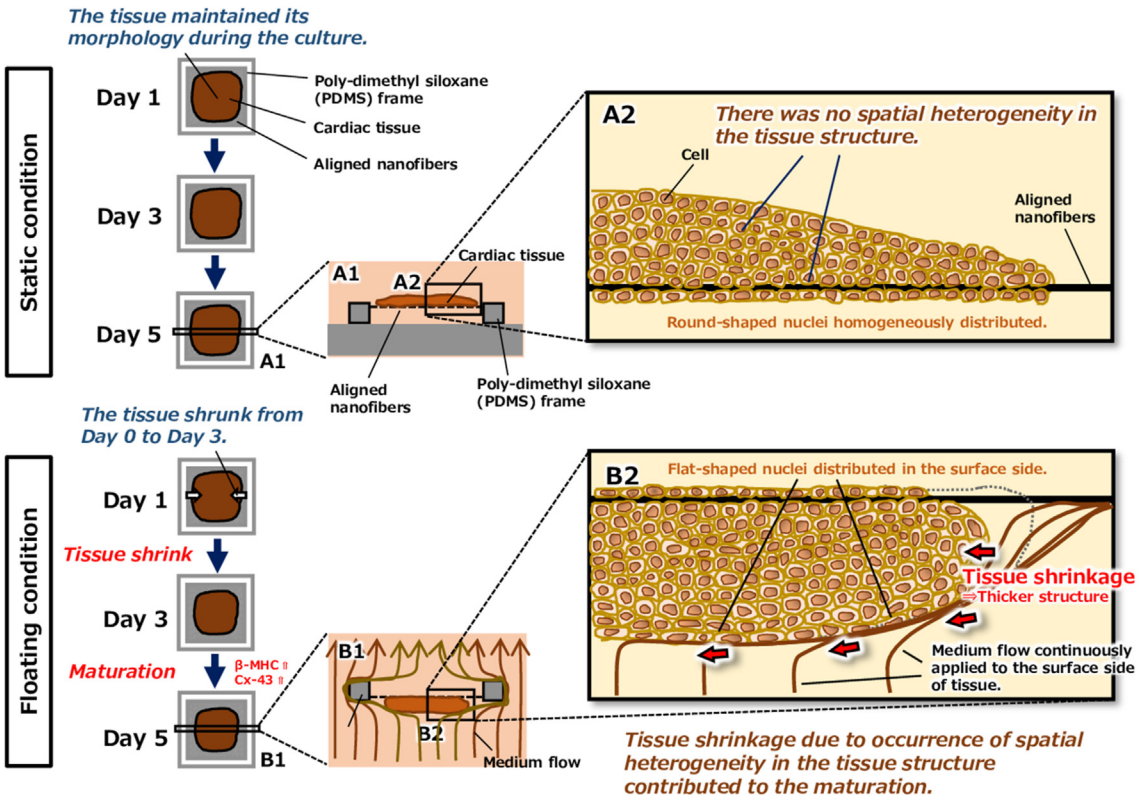

Fig. 6. Schematic illustration showing the maturation process of hiPSC-derived cardiac tissue in rotating flow culture. Comparing the time profile of tissue morphology and maturation marker proteins between these culture conditions, it was revealed that the tissue maturation in floating condition from Day 3 occurred after tissue shrinkage to become thicker structure from Day 0 to Day 3, suggesting the shrinkage was one of critical factors for tissue maturation. Moreover, compared with static condition, the tissue cultured in floating condition showed heterogeneous structure where flat-shaped nuclei distributed especially in the surface side of tissue. These findings show one of important characteristics of rotating flow culture for cardiac tissue maturation.

outside the cells via the cytoskeleton, and it regulates nuclei shape, chromatin structure, and gene expressions [46–49]. In the case of cardiomyocytes, Lamin A/C contributes to the formation of cardiac-specific cytoskeletal proteins and construction of sarcomere structures via activation of SUN1/2, nesprin, and desmin [39]. Moreover, the activation of these proteins is triggered by serum response factor (SRF), which is activated by the formation of Lamin A/C [39]. From these studies, it can be summarized that application of mechanical stress to cardiomyocytes plays an important role in cardiac maturation via the formation of the nuclear lamina Lamin A/C. In this study, the trigger of tissue shrinkage is considered to be the contractile force derived from actin-myosin movement in the surface region of the tissue, resulting that the mechanical force were given to the cells from the outside to the inside of the tissue. Moreover, tissue shrinkage also night contributed to the formation of Lamin A/C and cardiac maturation. These proposed mechanisms were also considered to coincide with the findings of previous study (Nakazato, et al.) [34], where the physiological hypertrophy of cardiomyocytes caused by medium flow of rotating flow culture was the critical phenomenon for tissue maturation.

These results also suggest that the important factor of rotating flow culture contributes to the maturation of cardiac tissue, which has remained unclear owing to the difficulty in defining this culture system for a long time. Many studies using this culture system have proposed possible mechanisms for tissue maturation, such as microgravity, infinite sedimentation, medium flow, and effective mass transport [26–33], but there is little evidence. Our study suggests the impact of medium flow in this culture system on morphological and structural changes in tissue, which critically affected the maturation of cardiac tissue. The role of mechanical stress on tissue maturation has been supported in many studies [19–21] but further understanding of the detailed mechanism is required in the future. This fundamental concept for understanding cardiac tissue maturation in rotating flow culture, with a focus on morphological and structural changes, might contribute not only to further understanding of the mechanism in different types of tissue, but also to the development of novel tissue culture techniques.

5. Conclusions

In this study, we demonstrated the maturation process of hiPSC-derived cardiac tissue in rotating flow culture by comparing the tissue morphology, structure, and maturation properties with those of static suspension culture. We found that spatial heterogeneity of tissue structure, which showed the distribution of flat-shaped nuclei in the surface region of tissue, and tissue shrinkage to become thicker structure occurred in rotating flow culture. Moreover, from the quantitative analysis for time profile of tissue morphology and cardiac maturation marker proteins, it was also suggested that tissue shrinkage contributed the following maturation of the tissue in rotating flow culture. These findings showed one of the important characteristics of rotating flow culture which was not revealed in previous studies.

Declaration of competing interest

There are no competing interests in the article titled “Effect of morphological change on the maturation of human induced

pluripotent stem cell-derived cardiac tissue in rotating flow culture", which we will submit in this time.

Acknowledgments

This research was supported by Project Focused on Developing Key Evaluation Technology: Development of Platform Technology for Drug Discovery through Application of Regenerative Medicine under grant number JP19be0604001, the Project Focused on Establishment of QbD-based control strategy and advanced core ecosystem in cell manufacturing under grant number JP20be0704001 from the Japan Agency for Medical Research and Development, Strategic Core Technology Advancement Program (Supporting Industry Program) (fiscal 2020), and Grant-in-Aid for JSPS Fellows (Grant Number 20J10116). The technical procedure for the bioreactor system was supported by JTEC Corporation in Japan. We also thank Dr. Nagako Sougawa (Department of Surgery, Division of Cardiovascular Surgery, Graduate School of Medicine, Osaka University) for technical supports of cardiac differentiation culture of hiPSCs.

Appendix A. Supplementary data

Supplementary data to this article can be found online at https://doi.org/10.1016/j.reth.2023.09.002.

References

[1] Martins AM, Vunjak-Novakovic G, Reis RL. The current status of iPS cells in cardiac research and their potential for tissue engineering and regenerative medicine. Stem Cell Rev Rep 2014;10:177–90.
[2] Miyagawa S, Sawa Y. Building a new strategy for treating heart failure using induced Pluripotent Stem Cells. J Cardiol 2018;72:445–8.
[3] Matsuura K, Wada M, Shimizu T, Haraguchi Y, Sato F, Sugiyama K, Konishi K, et al. Creation of human cardiac cell sheets using pluripotent stem cells. Biochem Biophys Res Commun 2012;425:321–7.
[4] Minami I, Yamada K, Otsuji TG, Yamamoto T, Shen Y, Otsuka S, et al. A small molecule that promotes cardiac differentiation of human pluripotent stem cells under defined, cytokine- and xeno-free conditions. Cell Rep 2012;2:1448–60.
[5] Mummery CL, Zhang J, Ng ES, Elliott DA, Elefanty AG, Kamp TJ. Differentiation of human embryonic stem cells and induced pluripotent stem cells to cardiomyocytes: a methods overview. Circ Res 2012;111:344–58.
[6] Matsumoto H, Ikuno T, Takeda M, Fukushima H, Marui A, Katayama S, et al. Human iPS cell-engineered cardiac tissue sheets with cardiomyocytes and vascular cells for cardiac regeneration. Sci Rep 2014;4:6716.
[7] Kawamura M, Miyagawa S, Fukushima S, Saito A, Miki K, Ito E, et al. Enhanced survival of transplanted human induced pluripotent stem cell-derived cardiomyocytes by the combination of cell sheets with the pedicled omental flap technique in a porcine heart. Circulation 2013;128:S87–94.
[8] Reiser PJ, Portman MA, Ning XH, Schomisch Moravec C. Human cardiac myosin heavy chain isoforms in fetal and failing adult atria and ventricles. Am J Physiol Heart Circ Physiol 2001;280:H1814–20.
[9] Lundy SD, Zhu WZ, Regnier M, Laflamme MA. Structural and functional maturation of cardiomyocytes derived from human pluripotent stem cells. Stem Cell Dev 2013;22:1991–2002.
[10] Karbassi E, Fenix A, Marchiano S, Muraoka N, Nakamura K, Yang X, et al. Cardiomyocyte maturation: advances in knowledge and implications for regenerative medicine. Nat Rev Cardiol 2020;17:341–59.
[11] Salameh A, Wustmann A, Karl S, Blanke K, Apel D, Rojas-Gomez D, et al. Cyclic mechanical stretch induces cardiomyocyte orientation and polarization of the gap junction protein connexin43. Circ Res 2010;106:1592–602.
[12] Han J, Wu Q, Xia Y, Wagner MB, Xu C. Cell alignment induced by anisotropic electrospun fibrous scaffolds alone has limited effect on cardiomyocyte maturation. Stem Cell Res 2016;16:740–50.
[13] Xu C, Wang L, Yu Y, Yin F, Zhang X, Jiang L, Qin J. Bioinspired onion epithelium-like structure promotes the maturation of cardiomyocytes derived from human pluripotent stem cells. Biomater Sci 2017;5:1810–9.
[14] Werner JC, Sicard RE, Schuler HG. Palmitate oxidation by isolated working fetal and newborn pig hearts. Am J Physiol 1989;256:E315–21.
[15] Lopaschuk GD, Spafford MA, Marsh DR. Glycolysis is predominant source of myocardial ATP production immediately after birth. Am J Physiol 1991;261:H1698–705.
[16] Stanley WC, Recchia FA, Lopaschuk GD. Myocardial substrate metabolism in the normal and failing heart. Physiol Rev 2005;85:1093–129.
[17] Matsuo T, Masumoto H, Tajima S, Ikuno T, Katayama S, Minakata K, et al. Efficient long-term survival of cell grafts after myocardial infarction with thick viable cardiac tissue entirely from pluripotent stem cells. Sci Rep 2015;5:16842.
[18] Sakaguchi K, Shimizu T, Horaguchi S, Sekine H, Yamato M, Umezu M, et al. In vitro engineering of vascularized tissue surrogates. Sci Rep 2013;3:1316.
[19] Russell B, Curtis MW, Koshman YE, Samarel AM. Mechanical stress-induced sarcomere assembly for cardiac muscle growth in length and width. J Mol Cell Cardiol 2010;48:817–23.
[20] Ruan JL, Tulloch NL, Razumova MV, Saiget M, Muskheli V, Pabon L, et al. Mechanical stress conditioning and electrical stimulation promote contractility and force maturation of induced pluripotent stem cell-derived human cardiac tissue. Circulation 2016;134:1557–67.
[21] Ronaldson-Bouchard K, Ma SP, Yeager K, Chen T, Song L, Sirabella D, et al. Advanced maturation of human cardiac tissue grown from pluripotent stem cells. Nature 2018;556:239–43.
[22] Li J, Minami I, Shiozaki M, Yu L, Yajima S, Miyagawa S, et al. Human pluripotent stem cell-derived cardiac tissue-like constructs for repairing the infarcted myocardium. Stem Cell Rep 2017;9:1546–59.
[23] Carrier RL, Rupnick M, Langer R, Schoen FJ, Freed LE, Vunjak-Novakovic G. Perfusion improves tissue architecture of engineered cardiac muscle. Tissue Eng 2002;8:175–88.
[24] Radisic M, Yang L, Boublik J, Cohen RJ, Langer R, Freed LE, et al. Medium perfusion enables engineering of compact and contractile cardiac tissue. Am J Physiol Heart Circ Physiol 2004;286:H507–16.
[25] Barash Y, Dvir T, Tandeitnik P, Ruvinov E, Guterman H, Cohen S. Electric field stimulation integrated into perfusion bioreactor for cardiac tissue engineering. Tissue Eng C Methods 2010;16:1417–26.
[26] Hammond TG, Hammond JM. Optimized suspension culture: the rotating-wall vessel. Am J Physiol Ren Physiol 2001;281:F12–25.
[27] Sladkova M, De Peppo GM. Bioreactor systems for human bone tissue engineering. Processes 2014;2:494–525.
[28] Varley MC, Markaki AE, Brooks RA. Effect of rotation on scaffold motion and cell growth in rotating bioreactors. Tissue Eng 2017;23:522–34.
[29] Okamura A, Zheng YW, Hirochika R, Tanaka J, Taniguchi H. In-vitro reconstitution of hepatic tissue architectures with neonatal mouse liver cells using three-dimensional culture. J Nanosci Nanotechnol 2007;7:721–5.
[30] Ishikawa M, Sekine K, Okamura A, Zheng YW, Ueno Y, Koike N, et al. Reconstitution of hepatic tissue architectures from fetal liver cells obtained from a three-dimensional culture with a rotating wall vessel bioreactor. J Biosci Bioeng 2011;111:711–8.
[31] Nishi M, Matsumoto R, Dong J, Uemura T. Engineered bone tissue associated with vascularization utilizing a rotating wall vessel bioreactor. J Biomed Mater Res 2013;101:421–7.
[32] Ohyabu Y, Kida N, Kojima H, Taguchi T, Tanaka J, Uemura T. Cartilaginous tissue formation from bone marrow cells using rotating wall vessel (RWV) bioreactor. Biotechnol Bioeng 2006;95:1003–8.
[33] Yoshioka T, Mishima H, Ohyabu Y, Sakai S, Akaogi H, Ishii T, et al. Repair of large osteochondral defects with allogeneic cartilaginous aggregates formed from bone marrow-derived cells using RWV bioreactor. J Orthop Res 2007;25:1291–8.
[34] Nakazato T, Kawamura T, Uemura T, Liu L, Li J, Sasai M, et al. Engineered three-dimensional cardiac tissues matured in a rotating wall vessel bioreactor remodel diseased hearts in rats with myocardial infraction. Stem Cell Rep 2022. https://doi.org/10.1016/j.stemcr.2022.03.012.
[35] Bianca CB, Kate LW, Lynette P, Julie RM. Molecular distinction between physiological and pathological hypertrophy: experimental findings and therapeutic strategies. Pharmacol Therapeut 2010;128:191–227.
[36] Shimizu I, Minamino T. Physiological hypertrophy and pathological hypertrophy. J Mol Cellular Cardiol 2016;97:245–62.
[37] Bray MA, Sheehy SP, Parker KK. Sarcomere alignment is regulated by myocyte shape. Cell Motil Cytoskeleton 2008;65:641–51.
[38] Kuo PL, Lee H, Bray MA, Geisse NA, Huang YT, Adams WJ, et al. Myocyte shape regulates lateral registry of sarcomeres and contractility. Am J Pathol 2012;181:2030–7.
[39] Carmosino M, Torretta S, Procino G, Gerbino A, Forleo C, Favale S, et al. Role of nuclear Lamin A/C in cardiomyocyte functions. Biol Cell 2014;106:346–58.
[40] Sougawa N, Miyagawa S, Sawa Y. Large-scale differentiation of human induced pluripotent stem cell-derived cardiomyocytes by stirring-type suspension culture. Methods Mol Biol 2021;2320:23–7.
[41] Hashida A, Uemura T, Kino-oka M. Kinetics on aggregate behaviors of human induced pluripotent stem cells in static suspension and rotating flow cultures. J Biosci Bioeng 2020;129:494–501.
[42] Koaykul C, Kim MH, Kawahara Y, Yuge L, Kino-oka M. Maintenance of neurogenic differentiation potential in passaged bone marrow-derived human mesenchymal stem cells under simulated microgravity conditions. Stem Cell Dev 2019;28:1552–61.
[43] Thanuthanakhun N, Kino-oka M, Borwornpinyo S, Ito Y, Kim MH. The impact of culture dimensionality on behavioral epigenetic memory contributing to pluripotent state of iPS cells. J Cell Physiol 2021;236:4985–96.
[44] Fukuda R, Gunawan F, Ramadass R, Beisaw A, Konzer A, Mullapudi ST, et al. Mechanical forces regulate cardiomyocyte myofilament maturation via the VCL-SSH1-CFL Axis. Dev Cell 2019;51:62–77.e65.
[45] Nakano K, Nanri N, Tsukamoto Y, Akashi M. Mechanical activities of self-beating cardiomyocyte aggregates under mechanical compression. Sci Rep 2021;11:15159.

[46] Lenz-Böhme B, Wismar J, Fuchs S, Reifegerste R, Buchner E, Betz H, et al. Insertional mutation of the Drosophila nuclear lamin Dm_0 gene results in defective nuclear envelopes, clustering of nuclear pore complexes, and accumulation of annulate lamellae. J Cell Biol 1997;137:1001–16.

[47] Sullivan T, Escalante-Alcalde D, Bhatt H, Anver M, Bhat N, Nagashima K, et al. Loss of A-type lamin expression compromises nuclear envelope integrity leading to muscular dystrophy. J Cell Biol 1999;147:913–20.

[48] Liu J, Rolef Ben-Shahar T, Riemer D, Treinin M, Spann P, Weber K, et al. Essential roles for Caenorhabditis elegans lamin gene in nuclear organization, cell cycle progression, and spatial organization of nuclear pore complexes. Mol Biol Cell 2000;11:3937–47.

[49] Dechat T, Gajewski A, Korbei B, Gerlich D, Daigle N, Haraguchi T, et al. LAP2alpha and BAF transiently localize to telomeres and specific regions on chromatin during nuclear assembly. J Cell Sci 2004;117:6117–28.